Int. J. Nanosci. Nanotechnol., Vol. 8, No. 1, March 2012, pp. 35-50

Application of Nano-Contact Mechanics Models in Manipulation of Biological Nano-Particle: FE Simulation

M. H. Korayem, Z. Rastegar

Robotic Research Laboratory, Center of Excellence in Exprimental Solid Mechanics and Dynamics, School of Mechanical Engineering, Iran University of Science and Technology, Tehran, I. R. Iran

(*) Corresponding author: hkorayem@iust.ac.ir
(Received:23 Nov. 2011 and Accepted: 05 Feb. 2012)

Abstract:
Contact mechanics is related to the deformation study of solids that meet each other at one or more points. The physical and mathematical formulation of the problem is established upon the mechanics of materials and continuum mechanics and focuses on computations involving bodies with different characteristics in static or dynamic contact. Contact mechanics gives essential information for the safe and energy efficient design of various systems. During manipulation process, contact forces cause deformation in contact region which is significant at nano-scale and affects the nano-manipulation process. Several nano-contact mechanics models such as Hertz, DMT, JKRS, BCP, MD, COS, PT, and Sun have been applied as the continuum mechanics approaches at nano-scale. Recent studies show interests in manipulation of biological cells which have different mechanical properties. Low young modulus and consequently large deformation makes their manipulation so sensitive. In this article small deformation contact mechanics models are used for biological cell, in air and liquid environment, then results will be compared with Tatara contact mechanics model which has been developed for hyperelastic materials with large deformation. Since biological cells are mostly modeled as visco- or hyper-elastic materials, this model will be more compatible with their condition. FE simulation has been done to investigate the applicability of these models and finite element approach in different ranges of deformations.
Keywords: *nano-contact mechanics models, biological cell, nano-manipulation, large deformation, FE simulation.*

1. INTRODUCTION

It is now well known that biological cells sense the mechanical changes in their environment. The outcoming response to mechanical changes is determinative in controlling the cell's action. The mechanical cell response is an intricate phenomenon. Realizing the mechanical behavior of the cell, first needs a precise knowledge of both force and stress distribution within the contact area. This feature is crucial since determining the force/ stress of various types of load can dictate the mechanical cell response. Moreover, to correlate the molecular biochemical interactions with the mechanical response of the cell, real time observation of cell development in order is required. Finally, mechanical cell characterization experiments need to be conducted in an in vitro environment so that the cell can be kept several hours in a living state for long experiments. Therefore, dependable and automatic measurements are needed to decrease human interference during the measurement process [17].

Pursuant to literature, much endeavor has been dedicated to recognize the mechanism by which the cell perceives the external mechanical actuations. In fact, so many methods have been developed, whether to mechanically stimulate

cells, sense force distributions or to determine the mechanical properties of the cells. Such as micropipette aspiration, atomic force microscopy, magnetocytometry or optical tweezers principles [18]. Among these methods, the most promising ones involve Scanning Probe Microscopy (SPM) techniques for the nano-scale level. These techniques have the potential to propone precise quantitative information relative to local forces and contact mechanics [17]. The Atomic Force Microscope (AFM) has become a commonly used tool in the field of bioscience.

The original work in contact mechanics dates back to 1882 with the publication of the paper "On the contact of elastic solids" by Heinrich Hertz. Hertz was trying to find out how the optical characteristics of multiple, stacked lenses might change with the force holding them together. Results in this field have since been expanded to all fields of engineering, but they are most essential in the study of tribology and indentation hardness. Hertzian contact stress refers to the localized stresses that develop as two curved surfaces come in contact and slightly deform under the imposed loads. This amount of deformation is dependent on the modulus of elasticity of the material in contact. It gives the contact stress as a function of the normal contact force, the radii of curvature of both bodies and the modulus of elasticity of both bodies [15].

It was not until nearly one hundred years later that Johnson, Kendall, and Roberts found a similar solution for the case of adhesive contact. This theory was rejected by Boris Derjaguin and co-workers who proposed a different theory of adhesion in the 1970s. The Derjaguin model came to be known as the DMT (after Derjaguin, Muller and Toporov) model, and the Johnson *et al.* model came to be known as the JKR (after Johnson, Kendall and Roberts) model for adhesive elastic contact. This rejection proved to be instrumental in the development of the Tabor and later Maugis parameters that quantify which contact model (of the JKR and DMT models) represent adhesive contact better for specific materials.

Further advancement in the field of contact mechanics in the mid-twentieth century may be attributed to Bowden and Tabor. Bowden and Tabor were the first to emphasize the importance of surface roughness for bodies in contact. The works of Bowden and Tabor yielded several theories in contact mechanics of rough surfaces [16].

However, these developments are confined to the case of small deformation and based on point or line contact of half-space elastic body model, and problems of large deformations in simple compression of elastic spheres as well as elastic bodies have remained unsolved. In 1991, Tatara proposed a new model which was the extension of Hertz mechanics model for hyper elastic material like rubber.

The organization of this article is as follows: interaction forces which are important in liquid environment are studied and their effects in contact mechanics models are applied. Then a comparison between small deformation contact models for gold nano-particle and biological nano-particle will be done. In addition Tatara large deformation model will be simulated for two different kind of biological cell and its results will be compared with small deformation models. Moreover, FE simulation will be done to investigate compatibility of contact mechanics models with finite element determination.

2- THEORY

2.1. Contact mechanics models

Contact mechanics models are used in different literature. But since these models have been developed for special conditions, their application in other situations would encounter problems and limitations. The Hertz model is the first contact mechanics model which does not consider the surface forces in contact, so if surface forces presents, this model is not appropriate for low loads. DMT theory considers a long-ranged surface force which acts outside the radius of the circle of contact, but contact geometry is similar to Hertzian. This model applies to rigid system with low λ, low adhesion and small radii of curvature, but may underestimate the true contact area. JKR considers a short-ranged surface force which acts inside the radius of the circle of contact. It applies to high λ systems, high adhesion and large radii of curvature, but may underestimate loading. Other important contact mechanics model is MD theory which considers the Dugdale potential to

describe attractive forces. It has analytical solution, but parametric equations. It applies to all system with all values of λ. But since this model is hard to use in complex system, other empirical and semi-empirical models such as BCP, COS, PT and SUN are developed to enhance the tractability of the MD model. These models are all applicable in small deformations, but there is another model which will be investigated in this paper as a large deformation model. this model invoke a non-linear elastic response and a large deformation formulation, however, it is the expanded Hertz theory for large deformation so it has some limitations. In this model the influence of adhesion and the effects of interfacial friction are not considered, but still seems to be an appropriate model to use in biological applications [16].

Small deformation models equations are widely used in other papers and their equations are given in appendix. However, Tatara model formulation as a suggested theory has been rarely used in other literature, so its formulae will be given in next section.

Tatara theory

The original Hertz model for a small deformation of a half-sphere of radius R_1 under compressive contact with a spherical probe of radius R_2 predicts that the force, F, depends on the 1.5th power of δ. In the subsequent formulas, subscript 1 and 2, respectively, denote the quantities for the sample and the tip, with common notations of E and ν, respectively, for Young's modulus and Poisson's ratio [19]

$$F = \frac{4}{3}\frac{\sqrt{R}E_1}{(1-\nu_1^2)}\delta^{3/2} = a\delta^{3/2} \quad (1)$$

Where $R=R_1R_2 / (R_1+R_2)$ and $a = \frac{4}{3}\frac{\sqrt{R}E_1}{(1-\nu_1^2)}$

In Tatara theory, by using the same symbol a as above, F is given as:

$$F = a\delta^{3/2} + \left(\frac{3a^2}{2a_c}\right)\delta^{3/2} + \left(\frac{15a^3}{8a_c^2}\right)\delta^{5/2} \quad (2)$$

Where $a_c = \frac{4\pi E_1 R_1}{(1+\nu_1)(3-2\nu_1)}$

2.2. Interaction forces

The DLVO theory states that the total interaction force (F_t) between two lyophobic particles in a medium can be expressed as a sum of the electrical double-layer force (F_e) and the van der Waals force (F_d) as follows:

$$F_t = F_e + F_d \quad (3)$$

The van der Waals force between two spheres of constant radii (R_1 and R_2 are treated as parameters) is then a function of separation (D) since the force on an object is the negative of the derivative of the potential energy function [1];

$$F_{VW}(D) = -\frac{dU(D)}{dD} \quad (4)$$

Yields:

$$F_{VW}(D) = -\frac{AR_1R_2}{(R_1+R_2)6D^2} \quad (5)$$

The van der Waals forces between objects with other geometries using the Hamaker model have been published in the literature. From the expression above, it is seen that the van der Waals force decreases with decreasing particle size (R). Accordingly, the van der Waals forces become prevailing for collections of very small particles such as very fine-grained dry powders (where there are no capillary forces present) even though the force of attraction is smaller in magnitude than it is for larger particles of the same substance.

A surface in a liquid may be charged by rupture of surface groups or by adsorption of charged molecules such as polyelectrolyte from the surrounding solution. This terminates in the development of a wall surface potential which will attract counterions from the surrounding solution and repel co-ions. In equilibrium, the surface charge is balanced by oppositely charged counterions in solution. The region near the surface of enhanced counterion concentration is called the electrical double layer (EDL). The EDL can be approximated by a sub-division into two regions. This immobile layer is called the Stern or Helmholtz layer. The region adjacent to the Stern layer is called

the diffuse layer and contains loosely associated ions that are comparatively mobile. The total electrical double layer due to the formation of the counterion layers results in electrostatic screening of the wall charge and minimizes the Gibbs free energy of EDL formation.

The thickness of the diffuse electric double layer is known as the Debye screening length1 / κ. At a distance of two Debye screening lengths, the electrical potential energy is reduced to 2 percent of the value at the surface wall [1].

$$\kappa = (\sum_i \rho_{\infty_i} > e^2 z_i^2 / \epsilon\epsilon_0 K_B T)^{1/2} \quad (6)$$

With unit of m^{-1} where

In which $\rho_{\infty i}$ is the number density of ion i in the bulk solution. Z is the valency of the ion. For example, H^+ has a valency of +1 and Ca^{2+} has a valency of +2. ϵ_0 is the electric constant, ε is the relative static permittivity, k_B is the Boltzmann constant and T is the temperature in Kelvin.

The repulsive free energy per unit area between two planar surfaces is shown as [11]

$$W = \left(\frac{64 K_B T \rho_\infty \gamma^2}{\kappa}\right) e^{-\kappa D} \quad (7)$$

Where:

γ is the reduced surface potential [11]

$$\gamma = \tanh\left(\frac{ze\psi_0}{4kT}\right) \quad (8)$$

ψ_0 is the potential on the surface.

The interaction free energy between two spheres of radius R is [11]

$$W = \left(\frac{64\pi k_B T R \rho_\infty \gamma^2}{\kappa^2}\right) e^{-\kappa D} \quad (9)$$

Combining the van der Waals interaction energy and the double layer interaction energy, the interaction between two particles or two surfaces in a liquid can be expressed as:

$$W(D) = W(D)_A + W(D)_R \quad (10)$$

Where $W(D)_R$ is the repulsive interaction energy due two electric repulsion and $W(D)_A$ is the attractive interaction energy due to van der Waals interaction. However, direct measurement of surface forces conducted in aqueous media showed the existence of forces not considered in the DLVO theory [12].

To sum up, although DLVO theory can be used in biological colloids, protein interactions are complicated because short-range forces have a significant impact on the rates and strengths of protein associations when involve, for example, hydration force. Therefore, in order to describe the solution behavior of proteins, DLVO theory and other forces' fields (e.g. non-DLVO forces) must be considered [4].

Hydration forces or solvation forces occur when molecules must overcome the obstacle caused by the water layer adsorbed on the surface of macromolecule. The energy for dislocating this water regulates the self-assembly of protein aggregates and other biomolecules. The raised intramolecular repulsion because of solvation layer is a well accepted phenomenon. Furthermore, the exclusion of water from protein interfaces stabilizes the interactions. This solvent mediate attraction is associated with the disruption of hydrogen bonds between water molecules by non-polar solutes [5]. From the imaging point of view, long-range interactions are probably less important, because these forces are likely to contribute only to a slowly varying background and to distribute over a large area on the specimen, resulting in small local deformations, provided that they are not very large in magnitude [9]. However, at short ranges, the hydration force (or solvation force in fluids other than water) is known to be important [10-12]

So the DLVO theory may be extended to include the contributions from the extraneous forces, as follows:

$$F_t = F_d + F_e + F_{hyd} \quad (11)$$

Where F_{hyd} represents the hydration force.

Different works for different electrolyte has been done. The work done by Grabbe and Horn 1993 showed that hydration force is slightly changed with the changes in surface treatment and electrolyte concentration. The measured hydration forces could be fitted to a double-exponential function of the form [13]:

$$\frac{F_{hyd}}{R} = C_1 e^{\left(-\frac{D}{D_1}\right)} + C_2 e^{\left(-\frac{D}{D_2}\right)} \qquad (12)$$

In which R is the tip radius, C_1, C_2, D_1 and D_2 are constants and D is the separation distance.

3- RESULTS

3.1. Contact mechanics models simulation results

Studies show that DNA can be considered as a nano-scale spherical pack [8] (Figure 1). So to simulate nano-scale biological cell behavior in contact moment, a pack of DNA was considered. Since bilological cells, such as DNA, live in biological environment, which is liquid, four different kinds of liquids are used to identify the effect of biological environment on DNA behavior. The liquid environment affects the interaction forces. So first of all forces in different liquids are simulated to find out the effectiveness of these forces in manipulation of biological cell in biological environment at the contact moment.

To calculate interaction forces some parameter are needed. One of these parameters is Hamaker constant which is calculated as follows [11]:

$$A \cong \frac{3}{4} K_B T \frac{(\varepsilon_1 - \varepsilon_3)(\varepsilon_2 - \varepsilon_3)}{(\varepsilon_1 + \varepsilon_3)(\varepsilon_2 + \varepsilon_3)} + \frac{3h}{4\pi} \cdot \int_{\nu_1}^{\infty} \left(\frac{\varepsilon_1(i\nu) - \varepsilon_3(i\nu)}{\varepsilon_1(i\nu) + \varepsilon_3(i\nu)}\right) \cdot \left(\frac{\varepsilon_2(i\nu) - \varepsilon_3(i\nu)}{\varepsilon_2(i\nu) + \varepsilon_3(i\nu)}\right) d\nu \qquad (13)$$

Where, K_B is Boltzman coefficient. T is temperature in Kelvin. ε_1 is dielectric constant for tip. ε_2 is dielectric constant for sample and ε_3 is dielectric constant for environment

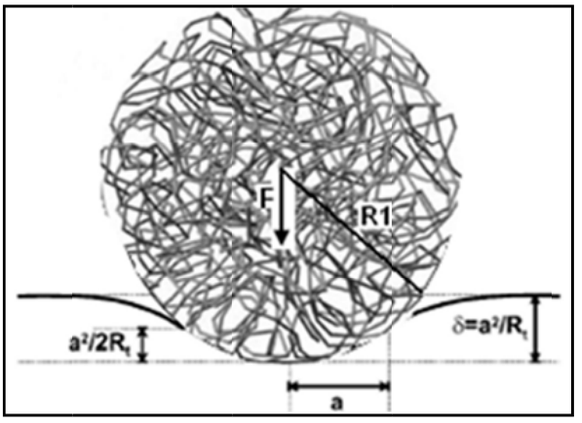

Figure 1: *Forced packing of a circular DNA*

The second part of the equation is ignorable. Calculated Hamaker constant for liquids are shown in Table 1.

Due to equation (12) calculating hydration foce for different liquids needs four constants, C_1,C_2,D_1 and D_2 (Table 2).

DNA and AFM tip properties are shown in Table 3.

Table 4. shows van der Waals force variations for different liquids in contact area. Contact moment in manipulation happens in about 0.165 nm. As shown in this figure, in this distance, the van der Waals force is approximately zero for these liquids. Since Hamaker constants for different liquids were approximately the same and have very small differences and forces' curves are similar. As mentioned before van der Waals force is dependent on Hamaker constant. As the data indicate, the van der Waals force for the liquid with smaller Hamaker constant is smaller .

Table 1: *Liquid properties*

	Dielectric coefficient	Hamaker constant (10^{-21})	Debye length (nm)
Water	80	2.64	96
Ethanol(10%)	74	2.61	176
Ethanol(20%)	69.5	2.58	196
Methanol	73.4	2.6	202

Table 2: *Hydration force constants [2]*

	C_1 (mN/m)	C_2 (mN/m)	D_1 (nm)	D_2 (nm)
Water	7.2	0.35	0.44	2.4
Ethanol(10%)	5	0.42	0.48	1.25
Ethanol(20%)	3.27	0.43	0.5	1.1
Methanol	8	0.35	0.41	2.3

Table 3: *DNA and AFM tip properties*

	Elasticity modulus(Gpa)	Poison ratio	Dielctric coeffeicient	σ (C/m^2)
DNA	0.1-0.2	0.35-0.5	2.56	0.16
AFM tip	169	0.27	3.9	0.025

Table 4: *Van der Waals forces vs. seperation distance*

Van der waals force (nN)	0.021 (nm)	0.0215 (nm)	0.022 (nm)
Water	8.53	8.21	7.87
Ethanol 10%	8.43	8.11	7.77
Ethanol 20%	8.33	8.01	7.67
Methanol	8.39	8.07	7.73

Table 5: *Hydration forces vs. seperation distance in different liquids*

Hydration force (nN)	0.02 (nm)	0.08 (nm)	0.16 (nm)
Water	0.121	0.105	0.0885
Ethanol 10%	0.0869	0.0765	0.0654
Ethanol 20%	0.0598	0.0531	0.0451
Methanol	0.133	0.115	0.095

Table 6: *Electrical double layer forcevs. seperation distance*

Electrical double layer force (N)	0.1 (nm)	0.2 (nm)
Water	$3.2085e10^{-10}$	$3.205\ e10^{-10}$
Ethanol 10%	$1.6196\ e10^{-13}$	$1.6187\ e10^{-13}$
Ethanol 20%	$1.36585\ e10^{-13}$	$1.3653\ e10^{-13}$
Methanol	$1.3998\ e10^{-13}$	$1.3991\ e10^{-13}$

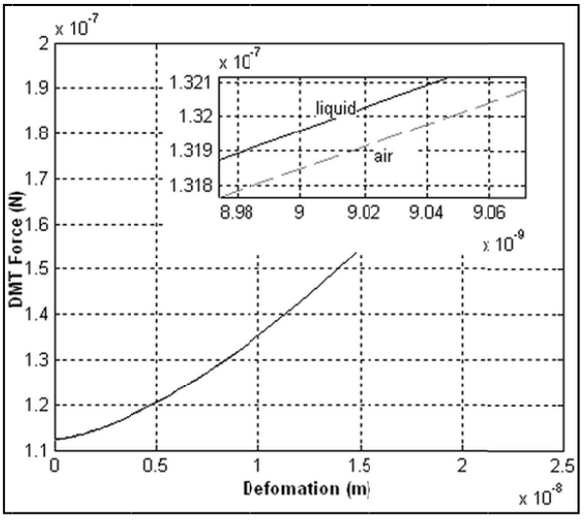

Figure 2: *DMT force (N) – deformation(m) curve in air and liquid*

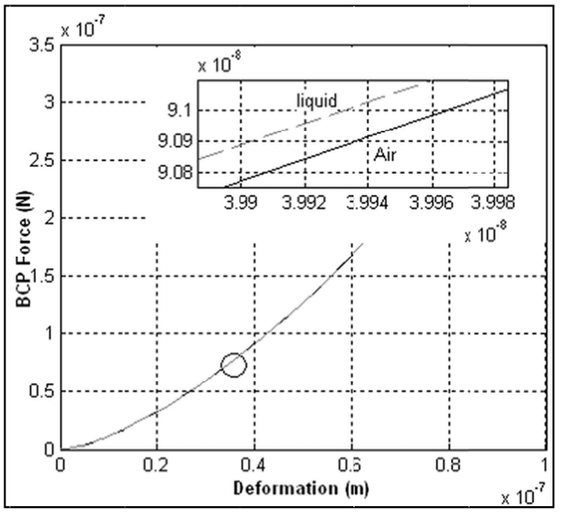

Figure 3: *BCP force (N) – deformation (m) curve in air and liquid*

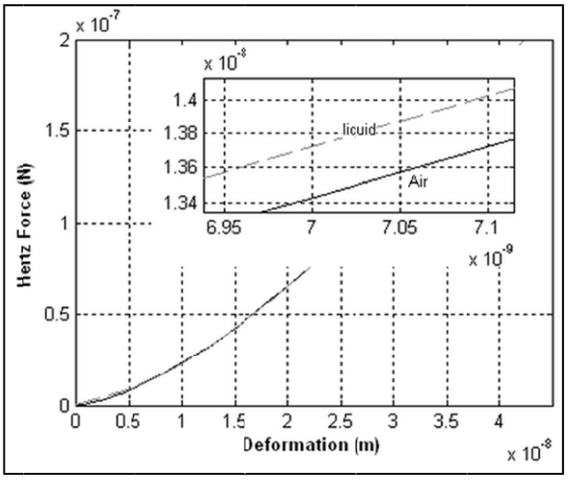

Figure 4: Hertz force(N)- deformation(m) curve in air (solid) and liquid (dash)

Table 5. illustrates hydration force variation for different liquids. As shown in the table 5. hydration forces decrease by increasing of distance, which results in ignorable hadration force at 0.165nm. the other considerable result is significant decrease in hydration force for ethanol 10% compared with water which shows the effect of concentration of the solvent on hydration force [2].

Table 6. show the electrical double layer forces in liquids. Again these forces are too small in contact moment to be considered.

Although it is found that these forces are too small to be considered in contact mechanics models, but forces were calculated and added to the external force to show the difference between results in liquid and air environment. Results are shown in Figures 2-4.

As expected, simulation shows that interaction forces calculated for fluid environment and added to the external force do not play an important role in manipulation and at the contact moment. So it can be concluded that contact mechanics models in liquid and air environment has ignorable differences. The same results were obtained for gold nano-particle [1]. Since most of interaction forces are repulsive, as shown in magnified figure to have the same deformation in fluid environment more force is needed to be applied than air.

To show differences between various contact mechanics models results for gold nano-particle and biological cell, simulation of contact moment for gold nano-particle and DNA has been done.

For both gold nano-particle and DNA, as shown in Figure 5 and 6, rising of pushing force results in increasing of indentation depth and contact area. Disregarding of adhesion force by Hertz theory results in underestimating of indentation depth. So this model cannot be used for all systems.

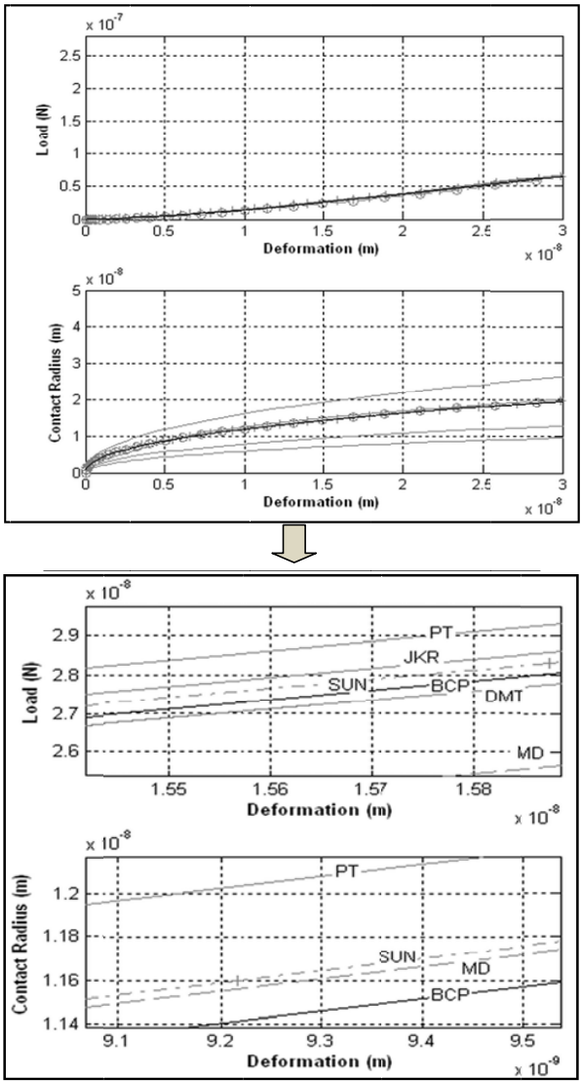

Figure 5: *Contact mechanics models for gold nano-particle*

It can be applied only for non-adhesive contacts with small deformation. In contrast JKR contact mechanics model considers the greatest adhesion force so the indentation depth obtained from this model is high. Consequently, JKR model provides the greatest contact area and the smallest contact radius is estimated by Hertz theory. DMT model has the lowest adhesion force. So this model is approximately similar to Hertz model and provides small indentation depth. BCP adhesion force and indentation depth is between JKR and DMT models. MD model does not have limitations of other models, so depending on deformation it's graph can fall down the other models' graphs. But since MD is an analytical model, other empirical models such as PT or COS which have more flexibility and easier calculation are used for complex systems.

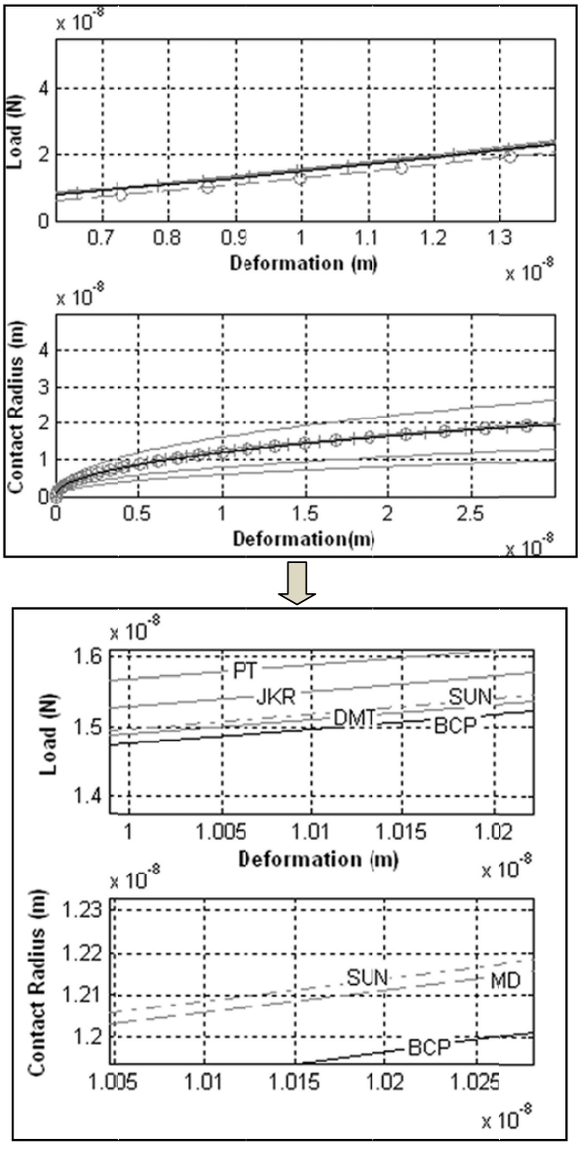

Figure 6: *Contact mechanics models for DNA*

Since Tatara theory is the expanded model of Hertz theory for hyper-elastic material, the comparison is done between these two models (Figure 7). Biological cells are usually modeled as a visco or hyper-elastic materials. Small deformation contact

mechanics models depict that whatever nano-particle becomes softer contact area rises while the applied load declines with sharp slope. But as mentioned before biological cells are visco or hyper-elastic materials and these kinds of materials have damping properties which does not let the material to deform so much due to small forces. Since Tatara theory as a large deformation model established for a hyper-elastic material, it is simulated for DNA.
Results show that using this model the slope of force- deformation curve is slower which is closer to the actual situation, so it is suggested to use this model for biological cell.
The same comparison is done for another biological cell whose experimental data are available. This comparison will prove our claim about validity of applying of Tatara model for biological cell. In this part a mouse embryonic stem cell is used. Its properties are shown in Table.7.

Table 7: *Mechanical properties of live mESM [14]*

	Live undiff
Diameter of the cell (μm)	10
Elastic modulus (Kpa)	0.169
Poisson ratio	0.49
Diameter of the tip	5

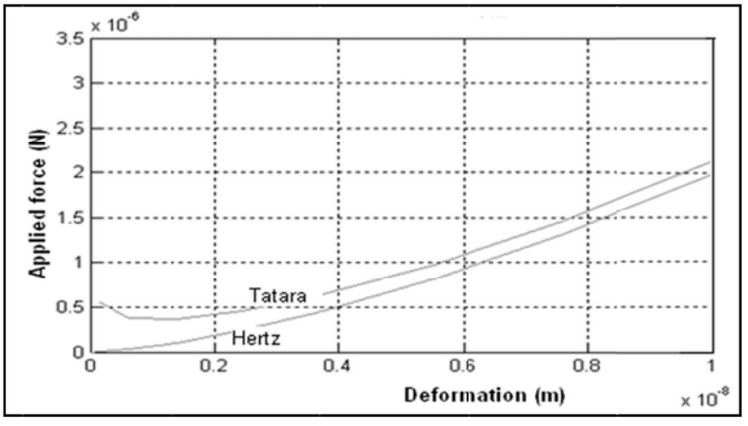

Figure 7: *Comparison of Tatara and Hertz models force(N)- displacement(m) curves for DNA*

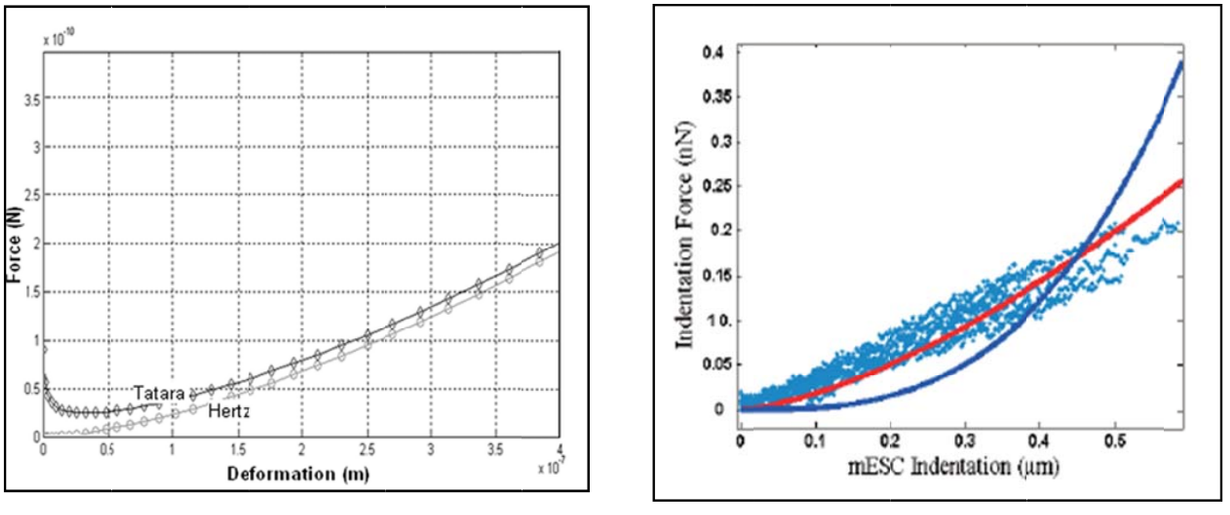

(a) (b)

Figure 8: *(a) Comparison of Tatara and Hertz models force(N)- displacement(m) curves for mESC (b) Exprimental curve [14]*

As it has been shown in Figure 8(a) Tatara model curve is more compatible with experimental data provided in Figure 13(b). The measured difference between experimental data and Tatara model is about 0.3% which is acceptable. This result for mESC proves that, as it mentioned before for DNA, Tatara contact mechanics model is more appropriate to use in analyzing biological cells behavior in contact moment and under applied load.

3.2. FE simulation results

In continuum mechanics, the mechanical properties of elastomeric materials are described in terms of a strain-energy density function W. If the left Cauchy-Green tensor is denoted by $B=FF^T$, where F is the gradient of deformation and λ_1, λ_2, λ_3 are the principal stretches, then, for an isotropic material, W is a function of strain invariants

$$I_1 = trB = \lambda_1^2 + \lambda_2^2 + \lambda_3^2,$$
$$I_2 = \frac{1}{2}[(trB)^2 - tr(B^2)] = \lambda_1^2\lambda_2^2 + \lambda_2^2\lambda_3^2 + \lambda_3^2\lambda_1^2,$$
$$I_3 = detB = \lambda_1^2\lambda_2^2\lambda_3^2 \qquad (14)$$

Rubber-like materials are often assumed to be incompressible provided that the hydrostatic stress does not become too large and so the admissible deformations must be isochoric, i.e., detF=1 so that I_3=1. The response of an incompressible isotropic elastic material can be determined by applying the standard constitutive law

$$T = -pI + 2\frac{\partial W}{\partial I_1}B - 2\frac{\partial W}{\partial I_2}B^{-1} \qquad (15)$$

Where p is a hydrostatic pressure term associated with the incompressibility constraint and T denotes the Cauchy stress. The classical strain-energy density for incompressible rubber is the Mooney-Rivilin Strain-energy

$$W = \frac{1}{2}\mu[\alpha(I_1 - 3) + (1 - \alpha)(I_2 - 3)] \quad (16)$$

Where $\mu>0$ is the constant shear modulus for infinitestimal deformations and $0< \alpha \leq 1$ is a dimensionless constant. when $\alpha=1$ in (49), one obtains the neo-Hookean strain-energy

$$W = \frac{\mu}{2}(I_1 - 3) \qquad (17)$$

Which corresponds to a Gaussian statistical mechanics model, and is often referred to as the kinetic theory of rubber. While the Mooney-Rivilin and neo-Hookean models are useful in describing rubber-like materials at small streches, the theorical predictions based on equations (16) and (17) do not adequately describe experimental data for rubber at high values of strain. For modeling of soft biological tissue, where rapid strain stiffening occurs even at moderate stretches, classical models are inappropriate.to model such stiffening, a number of alternative models have been proposed. In the molecular theory of elasticity these models are usually called non-Gaussian, because they introduce a distribution function for the end-to-end distance of the polymeric chain composing the rubber-like material which is not Gaussian. Such models are applicable to many other materials such as low-density polyethylenes, wool and chain fibers, and DNA molecules [20].

The finite element simulation is performed using ABAQUS 6.10. Following hyposesis are considered in FE modeling of biological cell:

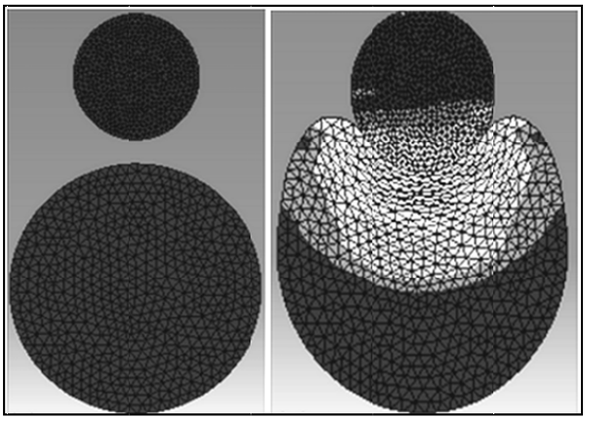

(a) (b)

Figure 9: *(a) Meshed model of AFM tip and spherical biological cell (b) Biological cell deformation after applying load by AFM tip*

1. The problem is axisymetric.
2. AFM tip is elastic (silicon).
3. The biological cell is supposed to be hemogenous, hyperelastic and incompressible material.

The part was meshed with 2786 triangular elements

(Figure 14(a)).
The result of biological cell deformation is shown in Figure 9(b). To compare FE simulation results with Hertz and Tatara model, force- deformation curve is extracted which is shown in Figure 10.

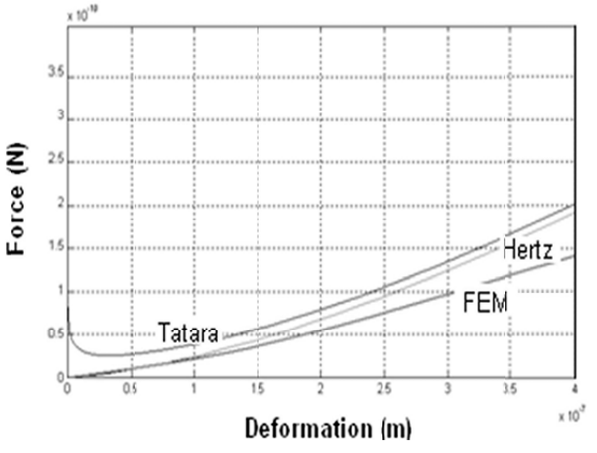

Figure 10: *Comparison between Tatara model, Hertz model and FEM simulation*

As shown in Figure 10 finite element simulation is in good agreement with Hertz theory and experimental data provided in Figure 8 (b) for small deformations but as indentation depth is increased the curves show significant difference. This result is similar to the results provided by Ladjal *et.al.*

4. CONCLUSION AND DISCUSSION

In this article, different small deformation contact mechanics models in manipulation of biological cell at contact moment were simulated. Since biological cells live in biological environment, four liquid in which biological cells can be kept were considered. Due to DLVO theory two major forces, van der Waals and electrical double layer forces, should be added to external force which is exerted by AFM tip. Although DLVO theory was proved to be practical for biological environment, literatures showed that non-DLVO forces such as hydration forces are also important. So, to modify contact mechanics models for biological condition three major forces were added to external force, van der Waals, electrical double layer and hydration forces. Contact moment of manipulation was simulated for nano-scale DNA of 50 nm radius submerged in pure water and three other biological fluids.
Results for van der Waals force shows that this force in every four fluids tends to zero in separation distance of 0.165 nm, so it can be ignored in contact theories. Electrical double layer and hydration forces are also ignorable due to their small values. Although forces' values were too small to be considered, they have been applied in JKR, DMT, Hertz and BCP theories and added to the external force to see the difference of this model in air and liquid environment. Results show that these theories for air and liquid environment are approximately the same. This conclusion is analogous to gold nano particle [1].
Small deformation contact mechanics models simulation results for DNA were compared with gold nano-particle. Since DNA is about 1000 times softer than gold nano particle, it was expected that larger deformations occur. Results comparison proved this idea. To deform gold nano-particle about 2.5×10^{-6}, 1000 times more force is needed in comparison with DNA.
Since Tatara theory is the expanded model of Hertz theory for hyper-elastic material, the comparison is done between these two models (Figure 7). Biological cells are usually modeled as a visco or hyper-elastic materials. Small deformation contact mechanics models depict that when the nano-particle becomes softer, contact area rises while the applied load declines with sharp slope. But as mentioned before, biological cells are visco or hyper-elastic materials and these kinds of materials have damping properties which does not let the material deform so much due to small forces; it means the force-deformation curve does not have sharp slope. Since Tatara theory as a large deformation model established for a hyper-elastic material, it is simulated for DNA. Results show that using this model the slope of force- deformation curve has slower trend which is closer to the actual situation, so it is suggested to use this model for biological cell. To verify the results obtained for DNA, simulation is done for mESC which experimental curve is available. Results' comparison in Figure 8 shows that Tatara theory is more compatible with experimental data.

Finite element simulation is done to compare its results with Hertz and Tatara model. Simulation results show agreement of finite element results with Hertz model in small deformations but for larger deformations its results are different.

Finally, it should be mentioned that for an accurate biological cell manipulation in liquid media, more studies about contact moment and deformations are needed. Since in vivo biological environment has different properties, study of contact moment and manipulation of biological cell in this environment can be more useful.

REFERENCE

1. M. H. Korayem,A. Motaghi, M. Zakeri, Dynamic modeling of submerged nanoparticle pushing based on atomic force microscopy in liquid medium, J Nanopart Res, Vol. 13, (2011), pp. 5009-5019.
2. R. Yoon, S. Vivek, Effects of Short-Chain Alcohols and Pyridine on the Hydration Forces between Silica Surfaces, Journal of Colloid and Interface Science Vol. 204, Issue 1, (1998), pp. 179-186.
3. C. Bustamante, S. B Smith, J. Liphardt, D. Smith, Single-molecule studies of DNA mechanics, Current Opinion in Structural Biology, Vol. 10, (2000), pp. 279-285.
4. D. Leckband, S. Sivasankar., Forces controlling protein interactions: theory and experiment, Colloid and Surfaces, B: Biointerfaces, Vol. 14, (1999), pp. 83-97.
5. J. Israelachvili, H. Weenerstrom, Role of hydration and water structure in biological and colloidal interactions, Nature, Vol. 379, (1996), pp. 219-227.
6. Jürgen Tomas, Mechanics of Particle Adhesion, 2004, D – 39106 Magdeburg, Germany.
7. E. J. Verwey, J. Th.G. Overbeek, Theory of the stability of lyophobic colloids, 1948, Amsterdam: Elsevier publishing company, ISBN 0-486-40929-5
8. J. Arsuaga, R. K. Z. Tanb, M. Vazqueza, D.W. Sumnersa, S. C. Harveyb, Investigation of viral DNA packaging using molecular mechanics models, Biophysical Chemistry, Vol. 101–102, (2002), pp. 475-484.
9. D. J. Muller, M. Baumeister, A. Engel, Conformational change of the hexagonally packed intermediate layer of Deinococcus radiodurans monitored by atomic force microscopy. J. Bacteriol. Vol. 178, (1996), pp. 3025-3030.
10. J. P. Cleveland, T. E. Schaffer, P. K. Hansma, Probing oscillatory hydration potentials using thermal-mechanical noise in an atomicforce microscope. Phys. Rev. B. Vol. 52, (1995), pp. 8692-8695.
11. J. N. Israelachvili, Intermolecular and Surface Forces, 1991, 2nd Ed. Academic Press, San Diego.
12. J. N. Israelachvili, R. M. Pashley, Molecular layering of water at surfaces and origin of repulsive hydration forces. Nature. Vol. 306, (1983), pp. 249-250.
13. A. Grabbe, R.G.J. Horn, Double-Layer and Hydration Forces Measured between Silica Sheets Subjected to Various Surface Treatment, Colloid Interface Sci. Vol. 157, (1993), pp. 375-383.
14. H. Ladjal, J-L Hanus, A. Pillarisetti, C. Keefer, A. Ferreira, J. P. Desai, Atomic Force Microscopy-Based Single-Cell Indentation: Experimentation and Finite Element Simulation, IEEE/RSJ International Conference onIntelligent Robots and Systems, (2009), pp. 1326-1332.
15. K. L. Johnson, Contact mechanics, 1985, Cambridge university press, 1st edition.
16. Y. Tatara, On compression of rubber elastic sphere over a large range of displacements, Journal of Engineering materials and Tchnology, Vol. 113, (1991), pp. 285-293.
17. M. Girot, M. Boukallel, S.Régnier, A hybrid microforce sensing device for mechanical cell characterization. In: Proc. of the Int. Conference on Instrumentation and Measurement Technology. (2006), pp. 501-506.
18. M. Lukkari, P. Kallio, Multipurpose impedancebased measurement system to automate microinjection of adherent cells. In: Proc. of the Int. Sympos. on Computational Intelligence in Robotics and Automation. (2005), pp. 20:26
19. A. Ikai, R. Afrin and H. Sekiguchi, Pulling and Pushing Protein Molecules by AFM, Current Nanoscience, Vol. 3, (2007), pp. 17-29
20. L. M. Kanner, Inflation of strain-stiffening rubber-like thin spherical shells, Biological Macromolecules Vol. 27, (2000), pp. 123:138.

Appendix

Hertz theory

As mentioned in Table.1 Hertz theory does not consider the surface forces and adhesion in contact. The relationship between applied load and indentation depth is given by following equations:

$$F = Ka\delta \qquad (A-1)$$

$$\delta = \frac{a^2}{\tilde{R}} \qquad (A-2)$$

Contact radius and adhesion force are obtained as follows:

$$a^3 = \frac{\tilde{\mathrm{R}}}{\mathrm{K}}\mathrm{F} \qquad (\mathrm{A}-3)$$

$$\mathrm{F_{ad}}=0 \qquad (A\text{ - }4)$$

JKR theory

The JKR theory model considers a short-ranged surface force which acts inside the contact area. The equations are as follows:

$$F = \frac{Ka^3}{\tilde{R}} - \sqrt{6\pi\omega Ka^3} \qquad (A-5)$$

$$\delta = \frac{a^2}{\tilde{R}} - \frac{2}{3}\sqrt{\frac{6\pi\omega a}{K}} \qquad (A-6)$$

$$a^3 = \frac{\tilde{R}}{K}\left(F + 3\pi\omega\tilde{R} + \left(6\pi\omega\tilde{R}F + \left(3\pi\omega\tilde{R}\right)^2\right)^{\frac{1}{2}}\right) \qquad (A-7)$$

$$F_{ad} = (6\pi\omega Ka^3)^{\frac{1}{2}} \qquad (A-8)$$

DMT theory

DMT model is the Hertz model with an offset due to surface forces. It considers a long-ranged surface force which acts outside the contact area but contact geometry is similar to the Hertz model. The equations are given as:

$$F = Ka\delta - 2\omega\tilde{R} \qquad (A-9)$$

$$\delta = \frac{a^2}{\tilde{R}} \qquad (A-10)$$

Contact radius and adhesion force are obtained as follows:

$$a^3 = \frac{\tilde{R}}{K}\left(F + 2\pi\omega\tilde{R}\right) \qquad (A-11)$$

$$F_{ad} = 2\pi\omega\tilde{R} \qquad (A-12)$$

MD theory

The MD theory model is more complex and more accurate than the other nano-contact mechanics models up to now. It considers the Dugdale (a step function) potential to describe attractive forces. The equations are:

$$F = \frac{Ka^3}{\tilde{R}} - \lambda a^2 \left(\frac{\pi\omega K^2}{\tilde{R}}\right)^{\frac{1}{3}} \left[\sqrt{m^2-1} + m^2 arctan\sqrt{m^2-1}\right] \qquad (A-13)$$

$$\delta = \frac{a^2}{\tilde{R}} - \frac{4\lambda a}{3}\left(\frac{\pi\omega}{\tilde{R}K}\right)^{\frac{1}{3}} \sqrt{m^2-1} \qquad (A-14)$$

$$\lambda = \frac{2.06}{\sigma}\left(\frac{\tilde{R}\omega^2}{\pi K^2}\right)^{\frac{1}{3}} \qquad (A-15)$$

$$m = \frac{c}{a} \qquad (A-16)$$

$$1 = \frac{\lambda a^2}{2}\left(\frac{K}{\pi\tilde{R}^2\omega}\right)^{\frac{2}{3}} \times \left[\sqrt{m^2-1} + (m^2-2)arctan\sqrt{m^2-1}\right] + \frac{4\lambda a^2}{3}\left(\frac{K}{\pi\tilde{R}^2\omega}\right)^{\frac{1}{3}} \times \left[1 - m + \sqrt{m^2-1}arctan\sqrt{m^2-1}\right] \qquad (A-17)$$

$$F_{ad} = \lambda a^2 \left(\frac{\pi\omega K^2}{\tilde{R}}\right)^{\frac{1}{3}} \times \left[\sqrt{m^2-1} + m^2 arctan\sqrt{m^2-1}\right] \qquad (A-18)$$

COS theory

Use of the MD theory is complicated by the indirect relationship between force and indentation; therefore, the COS empirical model has presented a solution for enhancing the tractability of the MD theory model by developing an empirical approximation of the relationship between contact radius and applied force. The equations are:

$$\frac{a}{a_0(\alpha)} = \left(\frac{a + \sqrt{1 + F/F_{ad}(\alpha)}}{1+\alpha}\right)^{\frac{2}{3}} \qquad (A-19)$$

$$\lambda = -0.924Ln(1 - 1.02\alpha) \qquad (A-20)$$

PT theory

The COS and PT equations provide the means to effectively apply the MD model to experimental data but the COS and PT models have more rapid calculations than the MD analytical model. The equations are:

$$\delta = \frac{a_0^2(\alpha)}{\tilde{R}}\left[\left(\frac{\alpha+\sqrt{1+F/F_{ad}(\alpha)}}{1+\alpha}\right)\right]^{\frac{4}{3}} - S(\alpha)\left(\frac{\alpha+\sqrt{1+F/F_{ad}(\alpha)}}{1+\alpha}\right)^{\frac{2}{3\beta(\alpha)}} \quad (A-21)$$

$$\lambda = -0.913Ln(1-1.018\alpha) \quad (A-22)$$

In which:

$$\tilde{a}_0(\alpha) = -0.451\alpha^4 + 1.417\alpha^3 - 1.365\alpha^2 + 0.950\alpha + 1.264 \quad (A-23)$$

$$\bar{F}_{ad}(\alpha) = 0.267\alpha^2 - 0.767\alpha + 2.000\,\alpha \quad (A-24)$$

$$S(\alpha) = -2.160\alpha^{0.019} + 2.7531\alpha^{0.064} + 0.073\alpha^{1.919} \quad (A-25)$$

$$\beta(\alpha) = 0.516\alpha^4 - 0.683\alpha^3 + 0.235\alpha^2 + 0.429\alpha \quad (A-26)$$

Sun Theory

the Sun model presents adhesive contact model for hyperboloid (blunted conical) indenters. The equations are:

$$F = \frac{3E^*}{2}\left\{\frac{A}{2\tilde{R}}\left[aA + \frac{a^2-A^2}{2}\left(\frac{\pi}{2} + arcsin\frac{(a/A)^2-1}{(a/A)^2+1}\right)\right] - a\left(\frac{8\pi a\omega}{3E^*}\right)^{\frac{1}{2}}\right\} \quad (A-27)$$

$$\delta = \frac{aA}{2\tilde{R}}\left(\frac{\pi}{2} + arcsin\frac{(a/A)^2-1}{(a/A)^2+1}\right) - \left(\frac{8\pi a\omega}{3E^*}\right)^{\frac{1}{2}} \quad (A-28)$$

In which:

$$A = R_t\cot(\varphi) \quad (A-29)$$

$$\delta$$

BCP theory

The BCP semiempirical model has been presented because the Hertz, DMT, and JKRS models did not match the experimental data. The equations are as follows:

$$F = \frac{Ka^3}{\tilde{R}} - \sqrt{\frac{3\pi\omega Ka^3}{2}} - \pi\omega\widetilde{R} \quad (A-30)$$

$$\delta = \frac{a^2}{\tilde{R}} - \left(\frac{\pi^2\omega^2\tilde{R}}{K^2}\right)^{\frac{1}{3}} \quad (A-31)$$

$$a^3 = \frac{\tilde{R}}{K}\left(F + \frac{7}{4}\pi\omega\tilde{R} + \left(\frac{33}{16}\left(\pi\omega\tilde{R}\right)^2 + \frac{3}{2}\left(\pi\omega\tilde{R}F\right)\right)^{\frac{1}{2}}\right) \quad (A-32)$$

$$F_{ad} = \left(\frac{3\pi\omega Ka^3}{2}\right)^{\frac{1}{2}} + \pi\omega\tilde{R} \quad (A-33)$$